Catalysis Science & Technology

ROYAL SOCIETY OF CHEMISTRY

PAPER

View Article Online
View Journal

Cite this: DOI: 10.1039/d6cy00473c

Mild and efficient coupling reactions enabled by *in situ* electrolytically generated Cu(I) cation catalyst in nanoelectrospray

Annesha Sengupta,[a] Gopal Reddy Ramidi,[a] Disni Gunasekera,[a] Mia Beaudoin,[a] Shiqing Xu [ab] and Xin Yan *[a]

Copper (Cu) catalysis merged with electrochemistry offers efficient transformations under mild conditions, yet *in situ* generation of active Cu species remains challenging. Here, we introduce a novel source of catalytically active Cu(I) cations that operates without strong additives, oxidants, high concentrations of Cu salts, bases, or elevated temperatures. These Cu(I) species are integrated into a nanoelectrospray ionization (nanoESI)-based electrocatalytic platform, in which a Cu wire replaces the conventional inert electrode. Under applied voltage, anodic corrosion releases Cu(I) directly into the reaction solution inside the emitter, providing (i) *in situ* generation of active Cu cations, (ii) electrocatalysis under additive-free mild conditions, and (iii) online reaction monitoring by high-resolution mass spectrometry (MS). The Cu electrode serves a dual role: as a sacrificial anode supplying Cu(I) without competing counteranions, enhancing reaction efficiency and minimizing MS signal suppression, and as a voltage source generating a stable electrospray for real-time analysis. Using this platform, we demonstrate efficient Cu-catalyzed (i) C–H amination of arenes, (ii) intermolecular N–N homocoupling of *o*-phenylenediamine, and (iii) intramolecular dehydrogenative N–N coupling of anthranilamide. The scalability of the electrochemical microreactor concept was demonstrated through the successful translation of the *in situ* Cu-catalyzed electrochemical C–H amination to a bulk electrochemical cell. This synergistic approach enables rapid reaction screening, discovery of mild conditions, and continuous capture of transient intermediates, providing novel mechanistic insight and advancing sustainable Cu electrocatalysis.

Received 11th April 2026,
Accepted 15th May 2026

DOI: 10.1039/d6cy00473c

rsc.li/catalysis

Introduction

Copper (Cu) catalysis has long been a cornerstone of synthetic chemistry, providing a cost-effective and earth-abundant alternative to noble transition metals. The versatility of copper, spanning oxidation states from 0 to +3, enables access to both single- and two-electron processes,[1,2] which underpin its success in diverse bond-forming reactions. In particular, Cu-catalyzed C–N and N–N coupling reactions are of great significance due to the ubiquity of nitrogen-containing motifs in natural products, pharmaceuticals, and functional materials.[3–5] Traditional approaches to Cu catalysis, however, typically rely on preformed complexes,[6] nanoparticles,[7] or Cu salts paired with ligands and additives.[8] These strategies, while powerful, often require harsh conditions, suffer from limited atom economy, and generate waste from ancillary reagents, highlighting the need for more sustainable catalytic platforms.[9,10]

Electrochemistry (EC) offers a sustainable alternative by replacing stoichiometric oxidants and reductants with electricity, thereby reducing by-product formation and improving atom economy.[11,12] Coupling novel EC techniques with mass spectrometric (MS) analysis, such as miniaturized three-electrode EC apparatus,[13] nanoelectrospray,[14] desorption electrospray,[15] nano-desorption spray,[16] neutral-reionization,[17] droplet spray,[18] plasma microdroplet fusion,[19] and microelectrochemical cell nanospray emitter,[20] has enabled the capturing of fleeting key intermediates for a better understanding of electrosynthetic pathways and has significantly contributed to designing environmentally friendly synthetic applications.[21,22]

The merger of electrocatalysis with transition-metal catalysis has proven to be a further powerful approach, enabling selective and efficient transformations under mild conditions.[11,23–33] In this context, the *in situ* generation of catalytically active cationic metal species has emerged as a particularly attractive strategy. Our group first demonstrated this concept for palladium: using nanoelectrospray ionization

[a] *Department of Chemistry, Texas A&M University, College Station, TX, USA. E-mail: xyan@tamu.edu*
[b] *Department of Pharmaceutical Sciences, Irma Lerma Rangel College of Pharmacy, Texas A&M University, College Station, TX, USA*

(nanoESI) as a controlled-current electrolytic (CCE) microreactor, the anodic corrosion of a Pd electrode produced cationic Pd species *in situ*, enabling mild and rapid C–C coupling and C–H arylation reactions.[27,34]

More broadly, electrospray ionization (ESI) functions as a CCE flow cell,[35–38] allowing electric current to serve as a "traceless" redox reagent that replaces traditional chemical oxidants and reductants.[39,40] In nanoESI, a wire-in-a-capillary bulk-loaded nanoESI emitter[41] is used, in which the embedded electrode acts as either an anode or a cathode in positive or negative ion modes, respectively.[38,42–44]

The palladium electrocatalytic platform developed by our lab further leveraged online mass spectrometry detection, facilitating real-time mechanistic studies at the picomole scale. The superior catalytic efficiency of anodically generated cationic Pd catalyst was further harnessed in scaled-up C–H arylation to achieve late-stage functionalization of drug molecules, confirming that the new electrochemical pathways discovered by nanoESI-MS can be translated to scalable electrosynthetic conditions.

Electrochemically generated metal ions have previously been studied to probe metal–ligand complexes,[41,45–47] the behavior of transition metal salts in electrospray,[48] and the formation of nanoparticles[43,49] or multi-metal 3D nanostructures.[50] However, *in situ* anodic formation of metal ions in ESI for simultaneous catalysis of chemical reactions remains rare.

Despite the central role of copper in catalysis, no analogous *in situ* Cu electrocatalytic systems have yet been developed. Existing methods for generating active Cu species rely on the reduction of Cu(II) or oxidation of Cu(0) in coordinating environments,[51] Cu–NHC complexes,[52] weakly coordinating anions,[6] or nanoparticles.[7] Although Cu salts have been integrated with ionization methods such as ESI[53–55] or DESI,[56] these systems have been primarily used to investigate Cu-catalyzed reaction mechanisms. However, none of these approaches electrolytically generated Cu cations *in situ* or demonstrated their catalytic activity.

In this work, we establish a novel Cu electrocatalytic platform based on nanoESI. By replacing the conventional inert nanoESI Pt electrode with a Cu wire, anodic corrosion under applied voltage releases catalytically active Cu(I) species directly into the reaction solution inside the emitter. This single-step setup unites (i) *in situ* generation of active Cu cations, (ii) electrocatalysis under mild conditions without extraneous ligands or additives, and (iii) online reaction monitoring by high-resolution MS.

In this setup (Fig. 1), the Cu electrode serves a dual role: it acts as a sacrificial anode that supplies catalytically active Cu cations without introducing competing counteranions or ligands, thereby improving reaction efficiency and minimizing signal suppression in MS analysis,[27,57,58] and simultaneously provides the voltage required to exceed the Rayleigh limit and generate a stable electrospray for online monitoring. Using this platform, we demonstrate efficient Cu-catalyzed (i) C–H amination of arenes, (ii) intermolecular N–N homocoupling of *o*-phenylenediamine, and (iii) intramolecular dehydrogenative N–N coupling of anthranilamide. Collectively, this synergistic approach advances sustainable Cu electrocatalysis while enabling rapid reaction discovery and mechanistic insight on the microscale.

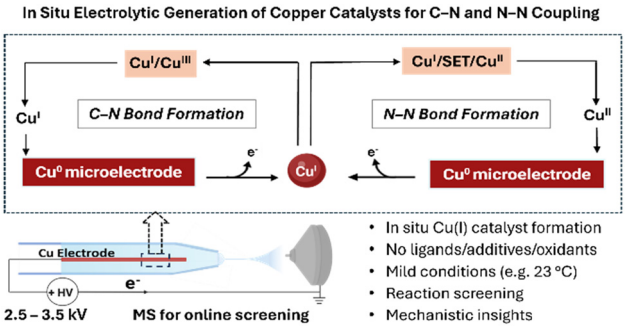

Fig. 1 Schematic of the nanoESI-based transition metal (TM) electrocatalytic microreactor for Cu-catalyzed C–N and N–N coupling. Catalytically active Cu(I) cations are generated *in situ via* anodic corrosion of a Cu wire in the nanoESI emitter. The same Cu electrode also generates a stable electrospray under applied voltage, transferring the reaction mixture to the mass spectrometer for online reaction screening and mechanistic analysis.

Results and discussion

In situ electrolytic generation of copper cations in nanoESI

We initiated probing the electrochemical generation of copper cations under nanoelectrospray conditions by examining the anodic corrosion of a copper wire electrode in a single-barrel nanoESI emitter. Upon applying a spray voltage of 2.0–2.5 kV, both electrochemical oxidation of the copper electrode and electrospray ionization were initiated simultaneously (Fig. S1). The threshold voltage required to generate Cu cations capable of coordinating ligands in solution and forming detectable Cu–ligand complexes was found to be approximately 0.02 kV (Fig. S2).

To determine the oxidation states of the anodically generated Cu species, nitrogen-containing ligands, including acetonitrile (ACN), 2-picolylamine (PA), 1,10-phenanthroline (1,10-Phen), and pyridine (Py), were introduced into the nanoESI emitter containing the copper electrode. Under these conditions, Cu(I) was identified as the predominant oxidation state for ligands such as ACN and Py, forming stable Cu(I)–ligand complexes readily detected by MS. In ACN, the major Cu(I) species included $[Cu(I)(H_2O)]^+$ (*m*/*z* 81.08), $[Cu(I)(ACN)]^+$ (*m*/*z* 104.08), $[Cu(I)(H_2O)(ACN)]^+$ (*m*/*z* 122.00), and $[Cu(I)(ACN)_2]^+$ (*m*/*z* 144.92) (Fig. 2d). In mixed Py/ACN solutions, these complexes were accompanied by $[Cu(I)(Py)]^+$ (*m*/*z* 141.97), $[Cu(I)(Py)(ACN)]^+$ (*m*/*z* 183.00), and $[Cu(I)(Py)_2]^+$ (*m*/*z* 221.01) (Fig. 2c).

Both Cu(I) and Cu(II) species were observed when stronger chelating ligands, such as 1,10-Phen and PA, were used (Fig. 2). In 1,10-Phen, electrolysis produced $[Cu(II)(1,10\text{-Phen})_2]^{2+}$ (*m*/*z* 211.58), $[Cu(I)(1,10\text{-Phen})]^+$ (*m*/*z* 243.00), $[Cu(I)(1,10\text{-Phen})(H_2O)]^+$ (*m*/*z* 261.00), and [Cu(I)

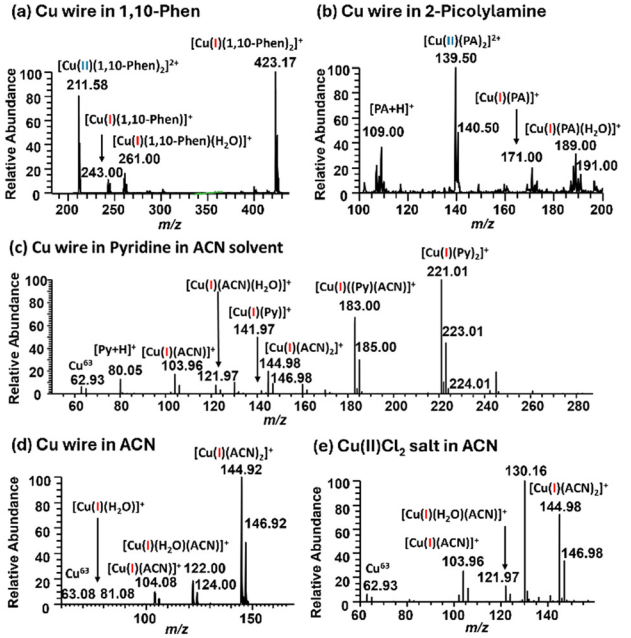

Fig. 2 Electrolysis of Cu electrode in nanoESI-MS (voltage: ~2.0 kV) to detect the stable Cu oxidation state in Cu-adducted ligands generated by anodic corrosion of Cu wire: (a) 1,10-phenanthroline in methanol solvent, (b) 2-picolylamine in methanol solvent, (c) pyridine in acetonitrile, (d) acetonitrile, and (e) Pt electrode in acetonitrile with $Cu(II)Cl_2$ as the source of Cu cations.

$(1,10\text{-Phen})_2]^+$ (*m*/*z* 423.17) (Fig. 2a). Similarly, in PA, the observed complexes included $[Cu(II)(PA)_2]^{2+}$ (*m*/*z* 139.50), $[Cu(I)(PA)]^+$ (*m*/*z* 171.00), and $[Cu(I)(PA)(H_2O)]^+$ (*m*/*z* 189.00) (Fig. 2b).

To further confirm the redox behavior, we compared these spectra to those obtained from electrospraying a $Cu(II)Cl_2$ solution (50 μM in ACN) using a platinum electrode. The resulting mass spectrum was identical to that produced from Cu electrode corrosion in ACN (Fig. 2e), indicating that Cu(II) ions are reduced to Cu(I) during the ESI process. Isotopic distribution patterns and tandem MS analyses (Fig. S3–S6) confirmed the identities and oxidation states of these Cu complexes. This gas-phase reduction likely arises from charge transfer and ligand desolvation events occurring within the spray plume.[44,48,59] This observation suggests the high preference of the nanoelectrospray environment for catalytically active Cu(I) species (see more discussion in S3).

These results demonstrate that anodic corrosion of copper in nanoESI can instantaneously produce both Cu(I) and Cu(II) cations without requiring strong acids or external oxidants. The resulting ions are stabilized by nitrogen-donor ligands, consistent with the Lewis acidic character of Cu(I)/Cu(II) as described by the HSAB principle.[49] This work emphasizes on Cu(I) as a major Cu-cationic species and primary catalytic contributor of all reactions. This is because, as observed in this study and reported in previous studies of anodic corrosion of Cu in nanoelectrospray settings, the presence and dominance of Cu(I) cations is a result of the comproportionation reaction. Cu(I) ions electrogenerated under these conditions can react directly with ligands.[60] This simple yet powerful platform captures the versatile redox chemistry of copper, capable of engaging in both one- and two-electron processes directly within the nanoESI environment.

Catalytic property of *in situ* electrolytically generated Cu(I) cations in nanoESI

Mild and efficient copper-catalyzed online electrochemical C–H amination. Cu(I) is known to have highly reactive and catalytic activity.[43,61–63] We next investigated whether the *in situ* anodically generated Cu(I) cations in nanoESI could have catalytic activity using the significant C–H amination of arene. The universality of N-containing motifs in pharmaceutical and natural products makes the development of efficient C–N coupling strategies indispensable. However, the strong nucleophilic nature of the parent amine poses a great challenge in achieving C–N coupling. C–H amination without C–H prefunctionalization thus often requires harsh reaction conditions.[10] Recent studies have reported an increasing demand in getting mechanistic insight into the catalytic C–H amination to aid in the discovery of practical and more environmentally benign conditions at room temperature to achieve the reaction.[64,65] Herein, we report accelerated and efficient C–H amination of arene at room temperature, catalyzed by *in situ* electrolyzed Cu(I) cations in nanoelectrospray, within 15 minutes of reaction initiation.

The electrochemical copper catalytic microreactor (orifice ~40 μm) was utilized to study the efficient C–H amination of non-pre-functionalized *N*-phenylpicolinamide (1, 250 μM) with morpholine (2, 4 equiv), utilizing potassium pivalate (KOPiv, 2 equiv), and tetra-*n*-butylammonium iodide (TBAI, 50 mol%) as the redox mediator in ACN solvent at room temperature (Fig. 3 and S7–S9). The Cu cations generated at a voltage application of 2.2–2.5 kV were utilized as the Cu catalyst. The electrochemical Cu-catalysis microreactor forms the C–N coupled product **3**, detected as $[\mathbf{3} + H]^+$ (*m*/*z* 284.14), $[\mathbf{3} + Na]^+$ (*m*/*z* 306.12), $[\mathbf{3} + K]^+$ (*m*/*z* 322.09), and $[Cu(I)(\mathbf{3}\text{-}H) + H]^+$ (*m*/*z* 346.06), after only 15 minutes, under mild reaction conditions and room temperature (Fig. 3f) (compared to bulk reaction requiring 24 hours).[65] The starting materials are seen as their protonated forms $[\mathbf{1} + H]^+$ at *m*/*z* 199.08 and $[\mathbf{2} + H]^+$ at *m*/*z* 88.07 (Fig. 3a). The limiting reagent $[\mathbf{1} + H]^+$ at *m*/*z* 199.08 disappears from the mass spectrum after 20 minutes (Fig. 3b), indicating its full consumption to form the Cu-mediated intermediates and C–N coupled product (see below).

Mechanistic insight into copper-catalyzed electrochemical C–H amination. The coupling of the nanoESI-based electrochemical transition metal microreactor with MS facilitates the study of the reaction mechanism by the detection and capturing of transient intermediates even at their low concentrations. Cu-catalyzed electrochemical C–H amination has been previously proposed to proceed through a Cu(II)/Cu(III) catalytic cycle involving single-electron transfer

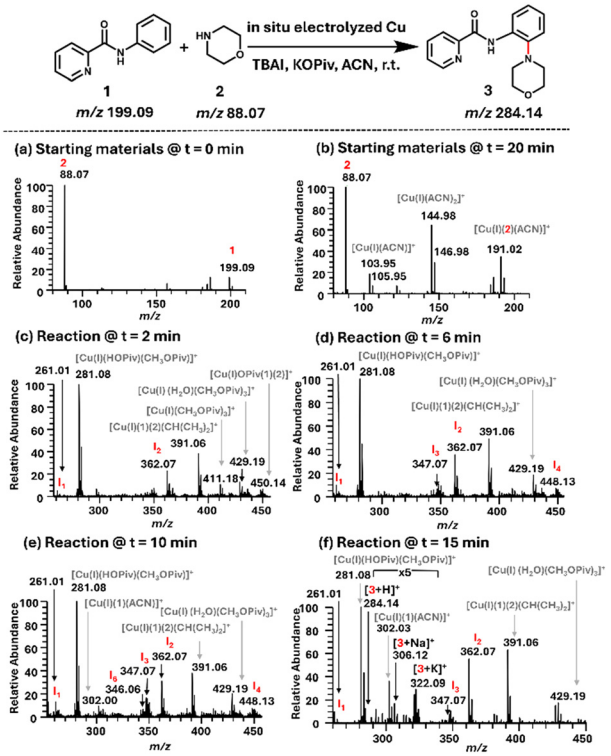

Fig. 3 C–H amination of *N*-phenylpicolinamide with morpholine in an electrochemical Cu catalytic microreactor at room temperature. Each spectrum represents the starting materials, intermediate, and products observed in the full MS at different time points: (a) starting materials, *N*-phenylpicolinamide (**1**) and morpholine (**2**) at time = 0 min; (b) the starting materials at time = 20 min, the limiting reagent **1** cannot be seen in the mass spectrum; (c) Cu(I) and Cu(II) intermediates $\mathbf{I_1}$ and $\mathbf{I_2}$ observed to form at time = 2 min; (d) Cu(II)-intermediate $\mathbf{I_3}$ and Cu(III)-intermediate $\mathbf{I_4}$ observed at time = 6 min; (e) Cu(I) C–N coupled intermediate $\mathbf{I_6}$ observed at *t* = 10 min; (f) product peaks, protonated [**3** + H]$^+$, sodiated [**3** + Na]$^+$, and potassiated [**3** + K]$^+$ seen at time = 15 min.

(SET),[3,65,66] including MS capture of fleeting intermediates, proposing the possibilities of two reductive elimination pathways, Cu(III)/Cu(I) and Cu(II)/Cu(0), responsible for driving the reaction.[54] Notably, we were able to capture multiple key intermediates, [Cu(I)(**1**-H) + H]$^+$ $\mathbf{I_1}$ at *m*/*z* 261.01, [Cu(II)(**1**-H) + H]$^{2+}$OPiv$^-$ $\mathbf{I_2}$ at *m*/*z* 362.06, [Cu(II)(**1**-H)(**2**)]$^{2+}$OPiv$^-$ $\mathbf{I_3}$ at *m*/*z* 347.07, [Cu(III)(**1**-H)(**2**)]$^{3+}$I$^-$OPiv$^-$ $\mathbf{I_4}$ at *m*/*z* 448.13, and [Cu(I)(**3**-H)]$^+$ at *m*/*z* 346.06 (Fig. 3c–f). The intermediates were detected in the positive ion mode of nanoESI-MS, carrying a single positive charge either due to an additional proton or charge on the Cu-cation.

From tracking the concentrations through extracted ion chromatogram (XIC), intermediates $\mathbf{I_1}$ (*m*/*z* 261.01), $\mathbf{I_2}$ (*m*/*z* 362.06), $\mathbf{I_3}$ (*m*/*z* 347.07), and $\mathbf{I_4}$ (*m*/*z* 448.13), start to form around 2 minutes and show increased stabilized intensity around 4 to 6 minutes; their concentration gradually decreases from 15 to 30 minutes. The C–N coupled intermediate bound to Cu(I) (*m*/*z* 346.06) starts to form around 5 minutes (detectable in MS at 10 minutes) and show increasing concentration along with the dominating product peaks [**3** + Na]$^+$ (*m*/*z* 306.12) and [**3** + K]$^+$ (*m*/*z* 322.09) over time from 15 to 30 minutes (Fig. S11). The intermediates were detected in the positive ion mode, catalyzed by Cu generated *in situ* by anodic corrosion. The intermediates were identified based on Cu isotopic distribution, XIC, and tandem MS (Fig. S12–S14).

Based on the experimental results, a plausible mechanism is proposed in Scheme 1. The reaction is initiated by the electrolysis of Cu(0) electrode in nanoESI, forming Cu(I) that reacts with **1** to form the Cu(I)-intermediate $\mathbf{I_1}$ (M + H at *m*/*z* 261.01), followed by the oxidation of Cu(I) and addition of pivalate to form the Cu(II)-intermediate $\mathbf{I_2}$ (M + H at *m*/*z* 362.06). $\mathbf{I_2}$ coordinates with **2**, yielding Cu(II)-intermediate $\mathbf{I_3}$ (M-OPiv at *m*/*z* 347.07). Further, the oxidation of Cu(II) forms a highly valent Cu(III) intermediate $\mathbf{I_4}$ (M-I at *m*/*z* 448.13) likely *via* oxidation by the iodine radical (Fig. S18). Cu(III)-species $\mathbf{I_4}$ undergoes SET to form Cu(II)-species $\mathbf{I_5}$, which is followed by intramolecular amine transfer and another SET to generate intermediate $\mathbf{I_6}$ (M + H at *m*/*z* 346.06). Alternatively, we cannot completely rule out that $\mathbf{I_4}$ may undergo ligand exchange in which the iodide is replaced by morpholine *via* HI loss, then followed by SET and intramolecular amine transfer to afford intermediate $\mathbf{I_6}$. $\mathbf{I_6}$ then releases the C–N coupled product **3** observed as [**3** + H]$^+$ (*m*/*z* 284.14), [**3** + Na]$^+$ (*m*/*z* 306.12), and [**3** + K]$^+$ (*m*/*z* 322.09), and regenerates a Cu(I) species.

The corresponding bulk reaction was performed in an undivided cell with the same reaction conditions as the online C–H amination reaction, but utilizing the traditional Cu catalyst, 10 mol% copper triflate (Cu(OTf)$_2$) (Fig. S15–S17).

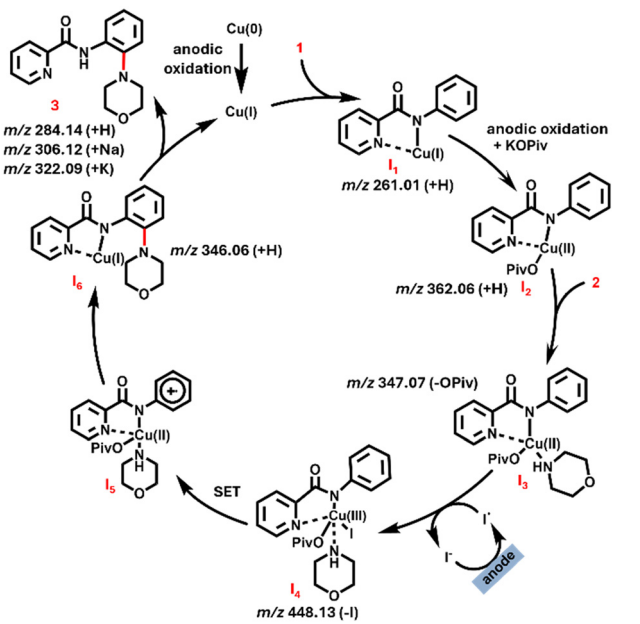

Scheme 1 Plausible catalytic cycle of Cu-catalyzed electrochemical C–H amination of *N*-phenylpicolinamide (**1**) with morpholine (**2**) supported by observed key Cu-intermediates in positive ion mode MS detection.

The product formation concentration was tracked over time and compared with the online C–H amination reaction catalyzed by the *in situ* electrolyzed Cu(I) cation. Comparing the reaction efficiency utilizing the conversion ratio of the limiting reagent transformed into intermediates and product, at 15 minutes, the *in situ* electrolyzed Cu catalyst achieved a ~99% conversion *versus* ~42% when catalyzed by a traditional Cu catalyst in bulk synthesis. The apparent acceleration factor, AAF (the intensity ratio of products and intermediates over reactants in the online microreactor *versus* bulk using the traditional Cu catalyst at the same reaction time),[67–70] was calculated to be ~314 (10^2 fold), which demonstrated the accelerated reaction utilizing the novel and efficient source of the *in situ* electrolytically generated Cu(I) catalyst in the online microreactor (Tables S1 and S2, eqn S1–S3).

Thus, the Cu-catalyzed electrochemical microreactor achieved accelerated C–H amination of arene at room temperature, serving as a highly efficient source of the Cu catalyst and as a reaction screening platform. Additionally, the microreactor enabled real-time capture of transient intermediates and products without signal suppression, providing mechanistic insight within just 15 minutes of reaction initiation.

Mild and efficient copper-catalyzed online electrochemical N–N homocoupling of *o*-phenylenediamine to form N-substituted benzotriazole. Excited by the result from C–H amination of arene, we next implemented the nanoESI-based Cu-catalyzed electrochemical microreactor to screen online electrochemical N–N coupling and aromatization of *o*-phenylenediamine to form a highly in-demand molecular moiety, benzotriazole.[71–73] Owing to the versatile use of N-substituted benzotriazoles in polymer materials, inhibitors, pesticides, and medicinal chemistry, there has been a vigorous development of their synthetic methods with special focus on eliminating harsh reaction conditions.[74,75] Herein, we report accelerated (4 minutes) N–N coupling and cyclization of *o*-phenylenediamine (**4**), under mild Cu-catalyzed electrochemical reaction conditions without base or oxidants, and at room temperature (previous conditions reporting use of strong base/high temperature),[74] yielding the significant benzotriazole moiety (Fig. 4).

The electrochemical-catalytic microreactor was utilized to study the efficient N–N intermolecular homocoupling and cyclization of *o*-phenylenediamine (**4**, 50 μM) in methanol solvent, catalyzed by *in situ* electrolytically generated Cu cations generated at a voltage of 2.5 kV in nanoESI. The activation of the highly nucleophilic amine group of the starting material **4** (*m*/*z* 109.08) by *in situ* generated Cu (Fig. 4a), led to the N–N dimerization, cyclization, and aromatization to yield the product, 2-(2*H*-benzotriazol-2-yl)benzenamine **5** (*m*/*z* 211.10) seen in full MS within 4 minutes of reaction initiation (Fig. 4c).

Mechanistic insight into copper-catalyzed electrochemical N–N homocoupling of *o*-phenylenediamine. Cu catalyzed

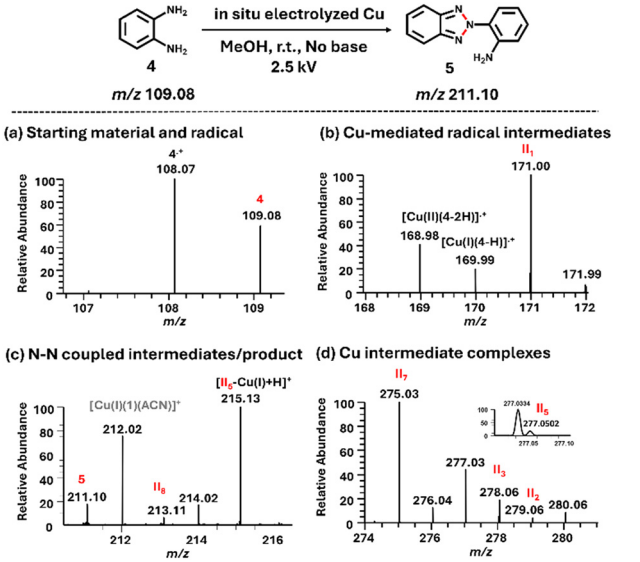

Fig. 4 N–N coupling of *o*-phenylenediamine (OPD) **4** to form 2-(2H-benzotriazol-2-yl)benzenamine **5** in the electrochemical Cu catalytic microreactor under mild reaction conditions and room temperature. Each spectrum represents the starting material, different intermediates, and products observed in the full MS over reaction time of 0 to 4 minutes: (a) mass spectrum showing the starting material **4** and radical $\mathbf{4}^{\bullet+}$; (b) Cu(I)-mediated intermediate $\mathbf{II_1}$, Cu(I) and Cu(II) radical complexes $[Cu(I)(\mathbf{4}\text{-H})]^{\bullet+}$ and $[Cu(II)(\mathbf{4}\text{-2H})]^{\bullet+}$; (c) N–N dimerized intermediate $[\mathbf{II_5}\text{-Cu(I)} + H]^+$, cyclized intermediate $\mathbf{II_8}$, and substituted benzotriazole product **5** formed in the nanoESI-based Cu-electrocatalytic microreactor; (d) Cu-mediated intermediate complexes $\mathbf{II_2}$–$\mathbf{II_7}$.

N–N dimerization has been previously proposed to navigate through Cu-mediated amine radical intermediates; however, a detailed understanding of the underlying mechanism remains limited.[74,76–79] Coupling of the nanoESI-based electrochemical transition metal microreactor with MS led to the unique capturing and detection of multiple fleeting intermediates, even at low concentrations, such as the Cu-complex intermediate $[Cu(I)(\mathbf{4})]^+$ $\mathbf{II_1}$ at *m*/*z* 170.99 (Fig. 4b), the dimerized intermediate $[\mathbf{II_5}\text{-Cu(I)} + H]^+$ (*m*/*z* 215.13), cyclized intermediate $\mathbf{II_8}$ (*m*/*z* 213.11) (Fig. 4c). The full MS spectrum was dominated by the Cu-complex intermediates $[Cu(I)(\mathbf{4})_2]^+$ $\mathbf{II_2}$ at *m*/*z* 279.06, $[Cu(II)(\mathbf{4}\text{-2H}) + H]^+$ $\mathbf{II_3}$ at *m*/*z* 278.06, $[Cu(I)(\mathbf{4}_2)]^+$ $\mathbf{II_5}$ at *m*/*z* 277.05, and $[Cu(II)(\mathbf{4}_2\text{-2H})]^{\bullet+}$ $\mathbf{II_7}$ at *m*/*z* 275.03 (Fig. 4d). The product **5** at *m*/*z* 211.10 was seen to be formed after 4 minutes of reaction initiation. This provided the unique opportunity to capture, analyse, and trace the intensity of every intermediate, giving mechanistic insight.

From tracking the concentrations through XIC, initial intermediate $\mathbf{II_1}$ at *m*/*z* 170.99 forms within a few seconds of voltage application and decreases after 4 minutes. Intermediates $\mathbf{II_2}$ (*m*/*z* 279.06), $\mathbf{II_3}$ (*m*/*z* 278.06), and $\mathbf{II_5}$ (*m*/*z* 277.05) form at 2 minutes and start to decrease at 4 minutes. At 4 minutes, the concentration of the intermediate $\mathbf{II_7}$ (*m*/*z* 275.03), and of product **5** (*m*/*z* 211.10) shows increasing concentration over time (Fig. S19). The structures were

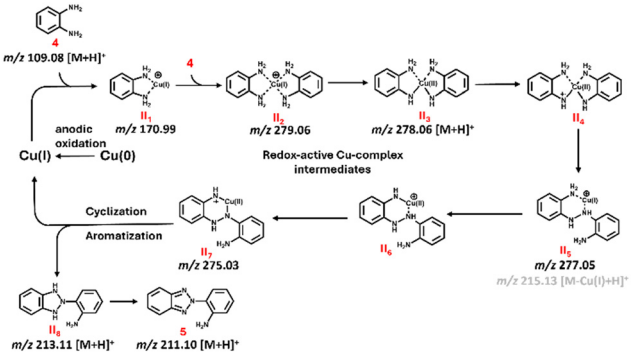

Scheme 2 Plausible reaction mechanism of Cu and electrolytically catalysed N–N coupling of *o*-phenylenediamine (**4**) to form 2-(2H-benzotriazol-2-yl)benzenamine (**5**) supported by observed key intermediates.

identified based on Cu isotopic distribution, high-resolution MS, and tandem MS (Fig. S20–S23, Table S3).

Based on the experimental results, a plausible mechanism is proposed in Scheme 2. The reaction is proposed to proceed through a series of redox-active Cu-complex intermediates.

Cu(0) undergoes anodic corrosion to form Cu(I) upon the application of voltage. Coordination of Cu(I) cation to one and two molecules of substrate **4** yields intermediate $\mathbf{II_1}$ (*m*/*z* 170.99) and the bis ligated Cu-complex intermediate $\mathbf{II_2}$ (*m*/*z* 279.06), respectively. Oxidative addition of the adducted amine groups to the Cu metallic center results in the Cu(II)-intermediate complex $\mathbf{II_3}$ (*m*/*z* 278.06). Cu-assisted N–H activation and SET is proposed to produce the Cu(II)-amine radical intermediate $\mathbf{II_4}$. Cu-mediated N–N coupling yields the dimerized intermediate $\mathbf{II_5}$ (*m*/*z* 277.05). A subsequent set of oxidative step generates the Cu(II)-complex $\mathbf{II_6}$, triggering SET at the remaining *ortho*-amine to form an N-centered radical $\mathbf{II_7}$ (*m*/*z* 275.03). Finally, **5** (*m*/*z* 211.10) is yielded from $\mathbf{II_7}$ from reductive elimination of Cu assisting N–N coupling, cyclization ($\mathbf{II_8}$, *m*/*z* 213.11), and aromatization. Radical trapping with 4 equivalents of (2,2,6,6-tetramethylpiperidin-1-yl)oxyl (TEMPO), resulted in negligible intermediates or no observation of product, confirming involvement of Cu-mediated redox active amine radical intermediates playing a key role in reaction progression (Fig. S25).

N–N homocoupling of *o*-phenylenediamine to form N-substituted benzotriazole catalyzed by *in situ* electrolyzed Cu cations in nanoESI was compared to the reaction catalyzed by a Cu(II)Cl_2 salt (60μmM) in nanoESI. The Cu-salt catalyzed spectrum generated an unstable signal (Fig. S24). For the Cu(II)Cl_2 catalyzed reaction, no radical Cu-mediated intermediates were observed with a conversion ratio of only ~11% achieved in 3 minutes, compared to ~64% when catalyzed by the *in situ* electrolyzed Cu catalyst, and a resulting AAF of ~15 (10 fold) (Fig. S25 and Tables S4 and S5).

Thus, with the application of the Cu-catalyzed electrochemical microreactor, online, fast and efficient N–N homocoupling of *o*-phenylenediamine was achieved in a novel metal-electrocatalytic system at room temperature without the use of any base.[74] This enabled the unique capture of intermediates and products without signal suppression and gave detailed mechanistic insight within just 4 minutes of the reaction initiation.

Mild and efficient copper-catalyzed online electrochemical dehydrogenative intramolecular N–N coupling of anthranilamide to form 3-indazolinone. With the achievement of N–N homocoupling of *o*-phenylenediamine, we were further motivated to test the N–N bond formation *via* the activation of the N–H bond of amides in the copper electrochemical microreactor. Recent synthetic efforts have seen an increasing focus on dehydrogenative catalytic methods to optimize the reaction conditions and alleviate the harsh conditions for the synthesis of the essential N-containing heterocycles.[80] However, activation of the inert N–H bond of amides still remains challenging and demands further exploration.[81–85] Herein, we report the dehydrogenative N–N coupling of anthranilamide to facilitate the facile construction of 3-indazolinone under mild reaction conditions (room temperature, in the absence of an oxidant), with the unique observation of key intermediates providing mechanistic insight.

The electrochemical Cu-catalytic microreactor was utilized to study the dehydrogenative intramolecular N–N coupling of anthranilamide (**6**, 200 μM) in methanol/water (1 : 1 v/v)

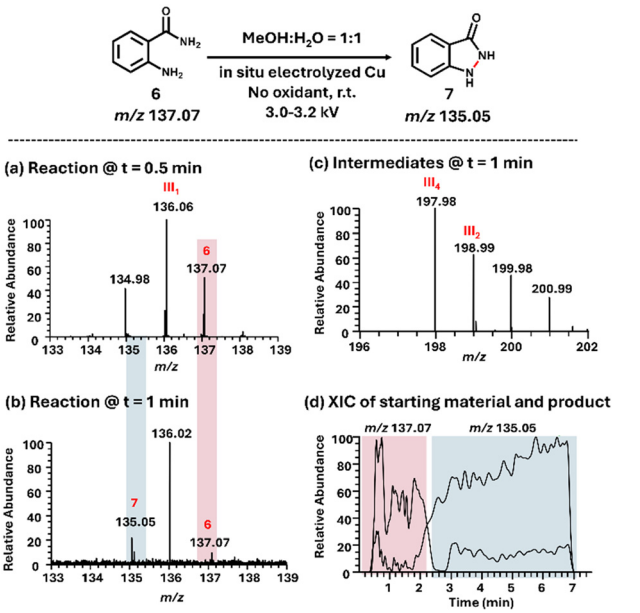

Fig. 5 Dehydrogenative intramolecular N–N bond formation of anthranilamide **6** to form 3-indazolinone **7** in an electrochemical Cu catalytic microreactor under mild reaction conditions, no oxidants, and at room temperature. Mass spectra showing (a) the starting material **6** and radical intermediate $\mathbf{III_1}$ at *t* = 0.5 min, (b) product 3-indazolinone **7** formed at *t* = 1 min, and (c) Cu(I)-intermediate $\mathbf{III_2}$ and Cu(I)-amine radical intermediate $\mathbf{III_4}$, and (d) XIC showing intensity of starting material **6** decreasing and product **7** increasing over a reaction time period of 7 minutes.

solvent, catalyzed by *in situ* electrolytically generated Cu cations generated at a voltage of 3.0–3.2 kV in nanoESI at room temperature without an oxidant (Fig. 5).

On application of voltage, the dehydrogenative intramolecular N–N coupled product, 3-indazolinone, **7**, was detected as $[7 + H]^+$ at *m*/*z* 135.05, in the full MS within 1 minute of the initiation of the reaction (Fig. 5a–c). The starting material, anthranilamide, **6** (*m*/*z* 137.07) initially seen as a dominant peak (Fig. 5a), gradually decreases with time (Fig. 5b). Tracking the intensities of **6** (*m*/*z* 137.07) and **7** (*m*/*z* 135.05) over time supports the observation of decreasing starting material intensity and increasing N–N coupled product intensity, as depicted in the XIC over a reaction period of 7 minutes under mild reaction conditions (without the use of oxidants and high temperature) (Fig. 5d).

Mechanistic insight into copper-catalyzed online electrochemical dehydrogenative intramolecular N–N coupling of anthranilamide. The dehydrogenative N–N coupling has been previously proposed to proceed *via* the Cu-catalyzed SET process and formation of a radical cation intermediate. However, the detailed SET process in the presence of the Cu catalyst is still unclear.[81] Our Cu electrocatalytic microreactor coupled with MS detection confirmed the mechanism by allowing the capture and characterization of unique and transient intermediates, adding detailed mechanistic insight (Fig. 5a–c). The key intermediate was found to be the radical intermediate $\mathbf{6}^{\bullet+}$ **III$_1$** at *m*/*z* 136.06, observed at 0.5 min, Cu(I)-adducted intermediate $[Cu(I)(\mathbf{6})]^+$ **III$_2$** at *m*/*z* 198.99 and Cu(I)-amine radical intermediate $[Cu(I)(\mathbf{6}\text{-H})]^{\bullet+}$ **III$_4$** at *m*/*z* 197.98, observed at 1 min after reaction initiation.

As observed from tracking intensities from the XIC, the concentration of starting material **6** (*m*/*z* 137.07) remains constant over the period of 2 minutes of reaction time. The radical intermediate **III$_1$** (*m*/*z* 136.06) and the Cu(I)-adducted intermediate $[Cu(I)(\mathbf{6})]^+$ **III$_2$** at *m*/*z* 198.99 initiate to form at 0.2 min, followed by the Cu(I)-amine radical intermediate $[Cu(I)(\mathbf{6}\text{-H})]^{\bullet+}$ **III$_4$** at *m*/*z* 197.98 at 0.3 min. The intensity of the product **7** at *m*/*z* 135.05 indicates it is slowly forming, with increasing intensity over the reaction time, and it dominates the starting material at *m*/*z* 137.07 at 1 minute (Fig. S26). The intermediates were identified based on Cu isotopic distribution, high-resolution MS, and tandem MS (Fig. S27 and S28, Table S6).

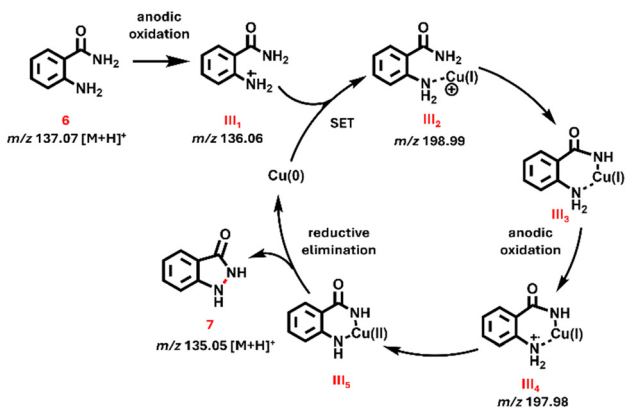

Scheme 3 Plausible reaction mechanism of Cu and electrolytically catalyzed dehydrogenative intramolecular N–N coupling of anthranilamide (**6**) to form 3-indazolinone (**7**) supported by observed key intermediates.

Based on the experimental results, a plausible mechanism is proposed in Scheme 3. Upon application of voltage, the starting material undergoes anodic oxidation to form radical intermediate **III$_1$** (*m*/*z* 136.06), which, followed by SET, forms the Cu(I)-intermediate **III$_2$** (*m*/*z* 198.99). Dehydrogenative coupling to Cu(I) followed by anodic oxidation generates the Cu(I) amine radical intermediate **III$_4$** (*m*/*z* 197.98). A subsequent SET and dehydrogenative coupling results in the Cu(II)-intermediate **III$_5$**, which, upon reductive elimination, yields the product **7** (*m*/*z* 135.05).

To confirm the radical-mediated pathway as the key contributor to the dehydrogenative intramolecular N–N coupling progression, the reaction was repeated in the presence of 3.5 equivalents of TEMPO to ensure sufficient radical capture (Fig. S29). In the presence of TEMPO, very little radical intermediate **III$_1$** (*m*/*z* 136.06) and **III$_4$** (*m*/*z* 197.98), and no product peak were observed after 1–3 min of 3 kV voltage application to the Cu electrode, confirming the key role of the radical intermediate. To further understand the role of the Cu catalyst, the reaction was repeated in the presence of a Pt inert electrode (3–3.5 kV). After 3 min of voltage application, no radical intermediate or product peaks were observed, strengthening the role of the Cu catalyst in initiating the radical mechanistic pathway coupled with the Cu-oxidative cycle to achieve the efficient N–N coupled product formation, yielding 3-indazolinone, **7**, from anthranilamide, **6**, under mild reaction conditions. (Fig. S29 and S30).

Thus, with the application of the Cu-catalyzed electrochemical microreactor, online and fast dehydrogenative intramolecular N–N coupling was achieved in a novel Cu-electrocatalytic system at room temperature without the use of any oxidant.[81] This enabled us to capture intermediates and products without signal suppression, providing rapid and unique mechanistic insight within 1 minute of the reaction initiation.

Scale-up of *in situ* Cu-catalyzed electrochemical C–H amination in an electrochemical cell. To demonstrate the feasibility of transferring the *in situ* generated Cu electrocatalyst system from nanoelectrospray to conventional bulk electrosynthesis, the scale-up of C–H amination of *N*-phenylpicolinamide **1** (0.4 mmol) with morpholine **2** (4 eq.) was performed with potassium pivalate (KOPiv, 2 equiv), and tetra-*n*-butylammonium iodide (TBAI, 50 mol%) in 4 ml ACN solvent at room temperature in an undivided cell with the Cu anode and Pt foil cathode. Cu anodic corrosion at a constant current of 10 mA was utilized to generate the *in situ* Cu catalyst within the electrochemical cell. The C–H aminated product **3** was obtained after 24 hours post purification in 45% yield. The product was characterized by ^{1}H NMR, ^{13}C

NMR, and HRMS (Fig. S32–S34). This scale-up experiment demonstrates that mechanistic and reactivity observations from the nanoESI platform can be successfully translated to bulk electrosynthesis, highlighting its value for rapid discovery of mild Cu-catalyzed electrochemical reactions.

Conclusions

In summary, we report a novel source of catalytically active Cu(I) cations and an electrochemical Cu-catalytic microreactor that can serve as a powerful platform for reaction screening and discovery of Cu-electrocatalytic reactions. Utilizing this novel platform, Cu-catalyzed electrochemical C–H amination of arene, N–N homocoupling and cyclization of phenyl diamine, and dehydrogenative N–N intramolecular coupling of amide were achieved in the absence of oxidants and additives, and at room temperature. The coupling of the electrochemical Cu microreactor with MS facilitated the real-time capturing of novel and transient intermediates, providing mechanistic insight within a few minutes of the reaction initiation. Possible catalytic cycles were proposed based on the observation of key intermediates. Furthermore, when compared with bulk electrosynthesis and with the nanoESI-based Cu catalytic microreactor utilizing traditional Cu salt as the catalyst, this platform achieved faster C–H amination and N–N homocoupling with an apparent acceleration factor of $\sim 10^2$-fold and ~10-fold, respectively, indicating the higher efficacy of the *in situ* electrolytically generated Cu(I) catalyst in the online microreactor. Further, the feasibility of transferring the *in situ* generated Cu electrocatalyst system from nanoelectrospray to bulk electrosynthesis was shown by the successful C–H amination in an undivided electrochemical cell. This approach enables novel Cu(I)-catalyzed electrocatalytic transformations, providing rapid mechanistic insights and thereby has the potential to significantly advance the field of transition metal electrocatalysis.

Author contributions

A. S., S. X., and X. Y. planned and designed the experiments. A. S. carried out experiments, performed the investigations, curated the data and wrote the manuscript. D. G., G. R. R., and M. B. carried out the investigations. X. Y. supervised the project and provided conceptual guidance. All authors contributed to manuscript writing, review, and editing.

Conflicts of interest

There are no conflicts to declare.

Data availability

Data will be made available upon request.

Supplementary information is available. See DOI: https://doi.org/10.1039/d6cy00473c.

Acknowledgements

The authors gratefully acknowledge the financial support from the NIH NIGMS (R35GM143047 to X. Y.), NSF (CHE 2145487 to X. Y.), the Welch grant (A-2089 to X. Y., grant A-2174 to S. X.), and the PRF (65298-DNI5 to X. Y.). The authors thank Pedro Martins Santucci for helpful discussions related to the electrochemical experiment setup.

Notes and references

1 S. E. Allen, R. R. Walvoord, R. Padilla-Salinas and M. C. Kozlowski, Aerobic copper-catalyzed organic reactions, *Chem. Rev.*, 2013, **113**(8), 6234–6458.
2 A. Verma and W. L. Santos, Copper-catalyzed coupling reactions of organoboron compounds, in *Boron Reagents in Synthesis*, ACS Publications, 2016, pp. 313–356.
3 S. Kathiravan, S. Suriyanarayanan and I. A. Nicholls, Electrooxidative Amination of sp2 C–H Bonds: Coupling of Amines with Aryl Amides via Copper Catalysis, *Org. Lett.*, 2019, **21**(7), 1968–1972, DOI: 10.1021/acs.orglett.9b00003.
4 M. C. Ryan, Y. J. Kim, J. B. Gerken, F. Wang, M. M. Aristov, J. R. Martinelli and S. S. Stahl, Mechanistic insights into copper-catalyzed aerobic oxidative coupling of N–N bonds, *Chem. Sci.*, 2020, **11**(4), 1170–1175.
5 J. B. Diccianni, C. Hu and T. Diao, N–N Bond Forming Reductive Elimination via a Mixed-Valent Nickel(II)–Nickel(III) Intermediate, *Angew. Chem., Int. Ed.*, 2016, **55**(26), 7534–7538, DOI: 10.1002/anie.201602566.
6 I. M. Riddlestone, A. Kraft, J. Schaefer and I. Krossing, Taming the cationic beast: novel developments in the synthesis and application of weakly coordinating anions, *Angew. Chem., Int. Ed.*, 2018, **57**(43), 13982–14024.
7 R. Pathak, V. D. Punetha, S. Bhatt and M. Punetha, A review on copper-based nanoparticles as a catalyst: synthesis and applications in coupling reactions, *J. Mater. Sci.*, 2024, **59**(15), 6169–6205.
8 Y. Tsuji and T. Fujihara, *Copper-based Catalysts*, 2015.
9 V. M. Breising, J. M. Kayser, A. Kehl, D. Schollmeyer, J. C. Liermann and S. R. Waldvogel, Electrochemical formation of N, N′-diarylhydrazines by dehydrogenative N–N homocoupling reaction, *Chem. Commun.*, 2020, **56**(31), 4348–4351.
10 H. Kim and S. Chang, Transition-Metal-Mediated Direct C–H Amination of Hydrocarbons with Amine Reactants: The Most Desirable but Challenging C–N Bond-Formation Approach, *ACS Catal.*, 2016, **6**(4), 2341–2351, DOI: 10.1021/acscatal.6b00293.
11 C. Ma, P. Fang, D. Liu, K.-J. Jiao, P.-S. Gao, H. Qiu and T.-S. Mei, Transition metal-catalyzed organic reactions in undivided electrochemical cells, *Chem. Sci.*, 2021, **12**(39), 12866–12873.
12 J. C. Siu, N. Fu and S. Lin, Catalyzing electrosynthesis: a homogeneous electrocatalytic approach to reaction discovery, *Acc. Chem. Res.*, 2020, **53**(3), 547–560.

13 K. Yu, H. Zhang, J. He, R. N. Zare, Y. Wang, L. Li, N. Li, D. Zhang and J. Jiang, In situ mass spectrometric screening and studying of the fleeting chain propagation of aniline, *Anal. Chem.*, 2018, **90**(12), 7154–7157.

14 Q. Wan, S. Chen and A. K. Badu-Tawiah, An integrated mass spectrometry platform enables picomole-scale real-time electrosynthetic reaction screening and discovery, *Chem. Sci.*, 2018, **9**(26), 5724–5729.

15 T. A. Brown, H. Chen and R. N. Zare, Identification of fleeting electrochemical reaction intermediates using desorption electrospray ionization mass spectrometry, *J. Am. Chem. Soc.*, 2015, **137**(23), 7274–7277.

16 P. Liu, I. T. Lanekoff, J. Laskin, H. D. Dewald and H. Chen, Study of Electrochemical Reactions Using Nanospray Desorption Electrospray Ionization Mass Spectrometry, *Anal. Chem.*, 2012, **84**(13), 5737–5743, DOI: 10.1021/ac300916k.

17 J. Liu, K. Yu, H. Zhang, J. He, J. Jiang and H. Luo, Mass spectrometric detection of fleeting neutral intermediates generated in electrochemical reactions, *Chem. Sci.*, 2021, **12**(27), 9494–9499, DOI: 10.1039/d1sc01385h.

18 H. Zhang, K. Yu, N. Li, J. He, L. Qiao, M. Li, Y. Wang, D. Zhang, J. Jiang and R. N. Zare, Real-time mass-spectrometric screening of droplet-scale electrochemical reactions, *Analyst*, 2018, **143**(18), 4247–4250.

19 A. J. Grooms, R. T. Huttner, M. Stockwell, L. Tadese, I. M. Marcelo, A. Kass and A. K. Badu-Tawiah, Programmable C–N Bond Formation through Radical-Mediated Chemistry in Plasma-Microdroplet Fusion, *Angew. Chem.*, 2025, **137**(4), e202413122.

20 R. Qiu, X. Zhang, H. Luo and Y. Shao, Mass spectrometric snapshots for electrochemical reactions, *Chem. Sci.*, 2016, **7**(11), 6684–6688, DOI: 10.1039/c6sc01978a.

21 A. Ingram, C. Boeser and R. Zare, Going beyond electrospray: mass spectrometric studies of chemical reactions in and on liquids, *Chem. Sci.*, 2016, **7**, 39–55.

22 A. K. Badu-Tawiah, L. S. Eberlin, Z. Ouyang and R. G. Cooks, Chemical aspects of the extractive methods of ambient ionization mass spectrometry, *Annu. Rev. Phys. Chem.*, 2013, **64**(1), 481–505.

23 F. Kakiuchi and T. Kochi, New strategy for catalytic oxidative C–H functionalization: Efficient combination of transition-metal catalyst and electrochemical oxidation, *Chem. Lett.*, 2020, **49**(10), 1256–1269.

24 K.-J. Jiao, Y.-K. Xing, Q.-L. Yang, H. Qiu and T.-S. Mei, Site-Selective C–H Functionalization via Synergistic Use of Electrochemistry and Transition Metal Catalysis, *Acc. Chem. Res.*, 2020, **53**(2), 300–310, DOI: 10.1021/acs.accounts.9b00603.

25 C. Ma, P. Fang and T.-S. Mei, Recent advances in C–H functionalization using electrochemical transition metal catalysis, *ACS Catal.*, 2018, **8**(8), 7179–7189.

26 C. Ma, P. Fang, Z.-R. Liu, S.-S. Xu, K. Xu, X. Cheng, A. Lei, H.-C. Xu, C. Zeng and T.-S. Mei, Recent advances in organic electrosynthesis employing transition metal complexes as electrocatalysts, *Sci. Bull.*, 2021, **66**(23), 2412–2429.

27 H. Cheng, T. Yang, M. Edwards, S. Tang, S. Xu and X. Yan, Picomole-Scale Transition Metal Electrocatalysis Screening Platform for Discovery of Mild C–C Coupling and C–H Arylation through in Situ Anodically Generated Cationic Pd, *J. Am. Chem. Soc.*, 2022, **144**(3), 1306–1312.

28 T. H. Meyer, L. H. Finger, P. Gandeepan and L. Ackermann, Resource economy by metallaelectrocatalysis: merging electrochemistry and CH activation, *Trends Chem.*, 2019, **1**(1), 63–76.

29 A. G. Wills, S. Charvet, C. Battilocchio, C. C. Scarborough, K. M. P. Wheelhouse, D. L. Poole, N. Carson and J. C. Vantourout, High-Throughput Electrochemistry: State of the Art, Challenges, and Perspective, *Org. Process Res. Dev.*, 2021, **25**(12), 2587–2600, DOI: 10.1021/acs.oprd.1c00167.

30 J. Rein, J. R. Annand, M. K. Wismer, J. Fu, J. C. Siu, A. Klapars, N. A. Strotman, D. Kalyani, D. Lehnherr and S. Lin, Unlocking the Potential of High-Throughput Experimentation for Electrochemistry with a Standardized Microscale Reactor, *ACS Cent. Sci.*, 2021, **7**(8), 1347–1355, DOI: 10.1021/acscentsci.1c00328.

31 S. Changmai, S. Sultana and A. K. Saikia, Review of electrochemical transition-metal-catalyzed C– H functionalization reactions, *ChemistrySelect*, 2023, **8**(11), e202203530.

32 J. Lu, Y. Wang, T. McCallum and N. Fu, Harnessing radical chemistry via electrochemical transition metal catalysis, *iScience*, 2020, **23**(12), 101796.

33 C. A. Malapit, M. B. Prater, J. R. Cabrera-Pardo, M. Li, T. D. Pham, T. P. McFadden, S. Blank and S. D. Minteer, Advances on the merger of electrochemistry and transition metal catalysis for organic synthesis, *Chem. Rev.*, 2021, **122**(3), 3180–3218.

34 M. E. Edwards, A. Sengupta, D. P. Freitas, E. A. Hirtzel, X. Chen, J. J. Kim and X. Yan, Interfacial electromigration for accelerated reactions, *Anal. Chim. Acta*, 2025, **1349**, 343854.

35 G. J. Van Berkel and F. Zhou, Electrospray as a controlled-current electrolytic cell: electrochemical ionization of neutral analytes for detection by electrospray mass spectrometry, *Anal. Chem.*, 1995, **67**(21), 3958–3964.

36 J. F. d. l. Mora, G. J. Van Berkel, C. G. Enke, R. B. Cole, M. Martinez-Sanchez and J. B. Fenn, Electrochemical processes in electrospray ionization mass spectrometry, *J. Mass Spectrom.*, 2000, **35**(8), 939–952.

37 G. S. Jackson and C. G. Enke, Electrical equivalence of electrospray ionization with conducting and nonconducting needles, *Anal. Chem.*, 1999, **71**(17), 3777–3784.

38 A. T. Blades, M. G. Ikonomou and P. Kebarle, Mechanism of electrospray mass spectrometry. Electrospray as an electrolysis cell, *Anal. Chem.*, 1991, **63**(19), 2109–2114.

39 J. Liu, L. Lu, D. Wood and S. Lin, New redox strategies in organic synthesis by means of electrochemistry and photochemistry, *ACS Cent. Sci.*, 2020, **6**(8), 1317–1340.

40 S. Möhle, M. Zirbes, E. Rodrigo, T. Gieshoff, A. Wiebe and S. R. Waldvogel, Modern electrochemical aspects for the synthesis of value-added organic products, *Angew. Chem., Int. Ed.*, 2018, **57**(21), 6018–6041.

41 G. J. Van Berkel, K. G. Asano and P. D. Schnier, Electrochemical processes in a wire-in-a-capillary bulk-

loaded, nano-electrospray emitter, *J. Am. Soc. Mass Spectrom.*, 2001, **12**(7), 853–862.
42 D. Freitas, X. Chen, H. Cheng, A. Davis, B. Fallon and X. Yan, Recent Advances of In-Source Electrochemical Mass Spectrometry, *ChemPlusChem*, 2021, **86**(3), 434–445.
43 A. Li, Q. Luo, S. J. Park and R. G. Cooks, Synthesis and catalytic reactions of nanoparticles formed by electrospray ionization of coinage metals, *Angew. Chem., Int. Ed.*, 2014, **53**(12), 3147–3150.
44 C. J. Pulliam, R. M. Bain, H. L. Osswald, D. T. Snyder, P. W. Fedick, S. T. Ayrton, T. G. Flick and R. G. Cooks, Simultaneous online monitoring of multiple reactions using a miniature mass spectrometer, *Anal. Chem.*, 2017, **89**(13), 6969–6975.
45 J. Yin, H. Zhang, M. Luo, J. Zhao, B. Huang, P. Chen, Z. Cai, Y. Yuan, Y. Liu and C. He, Regulating the dominant reactive oxygen species from Fe (IV)-oxo to 1O2 by deprotonation of Fe (IV)-oxo in electro-Fe (II)/periodate system, *Chem. Eng. J.*, 2024, **497**, 154896.
46 V. Katta, S. K. Chowdhury and B. T. Chait, Electrospray ionization: a new tool for the analysis of ionic transition-metal complexes, *J. Am. Chem. Soc.*, 1990, **112**(13), 5348–5349.
47 A. T. Blades, P. Jayaweera, M. G. Ikonomou and P. Kebarle, First studies of the gas phase ion chemistry of M3+ metal ion ligands, *Int. J. Mass Spectrom. Ion Processes*, 1990, **101**(2–3), 325–336.
48 J. J. Boock and R. A. Yost, Behavior of transition metal salts during the electrospray ionization process, *Int. J. Mass Spectrom.*, 2019, **446**, 116217.
49 A. Li, Z. Baird, S. Bag, D. Sarkar, A. Prabhath, T. Pradeep and R. G. Cooks, Using Ambient Ion Beams to Write Nanostructured Patterns for Surface Enhanced Raman Spectroscopy, *Angew. Chem., Int. Ed.*, 2014, **53**(46), 12528–12531, DOI: 10.1002/anie.201406660.
50 A. Reiser, M. Lindén, P. Rohner, A. Marchand, H. Galinski, A. S. Sologubenko, J. M. Wheeler, R. Zenobi, D. Poulikakos and R. Spolenak, Multi-metal electrohydrodynamic redox 3D printing at the submicron scale, *Nat. Commun.*, 2019, **10**(1), 1853, DOI: 10.1038/s41467-019-09827-1.
51 C. Sambiagio, S. P. Marsden, A. J. Blacker and P. C. McGowan, Copper catalysed Ullmann type chemistry: from mechanistic aspects to modern development, *Chem. Soc. Rev.*, 2014, **43**(10), 3525–3550.
52 F. Lazreg, F. Nahra and C. S. Cazin, Copper–NHC complexes in catalysis, *Coord. Chem. Rev.*, 2015, **293**, 48–79.
53 K. Iyer, J. Yi, A. Bogdan, N. Talaty, S. W. Djuric and R. G. Cooks, Accelerated multi-reagent copper catalysed coupling reactions in micro droplets and thin films, *React. Chem. Eng.*, 2018, **3**(2), 206–209, DOI: 10.1039/c8re00002f.
54 M. Kumar, S. Verma, A. Kumar, P. K. Mishra, R. O. Ramabhadran, S. Banerjee and A. K. Verma, Mechanistic insights of Cu (ii)-mediated ortho-C–H amination of arenes by capturing fleeting intermediates and theoretical calculations, *Chem. Commun.*, 2019, **55**(63), 9359–9362.
55 J. Ghosh and R. G. Cooks, Facile Synthesis of Triazoles using Electrospray-Deposited Copper Nanomaterials to Catalyze Azide-Alkyne Cycloaddition (AAC) Click Reactions, *ChemPlusChem*, 2022, **87**(10), e202200252.
56 S. Banerjee, S. Sathyamoorthi, J. Du Bois and R. N. Zare, Mechanistic analysis of a copper-catalyzed C–H oxidative cyclization of carboxylic acids, *Chem. Sci.*, 2017, **8**(10), 7003–7008, DOI: 10.1039/c7sc02240a.
57 A. Sengupta, M. E. Edwards and X. Yan, Dual metal electrolysis in theta capillary for lipid analysis, *Int. J. Mass Spectrom.*, 2023, **494**, 117137.
58 S. Tang, X. Chen, Y. Ke, F. Wang and X. Yan, Voltage-controlled divergent cascade of electrochemical reactions for characterization of lipids at multiple isomer levels using mass spectrometry, *Anal. Chem.*, 2022, **94**(37), 12750–12756.
59 D. Płonka, R. Kotuniak, K. Dabrowska and W. Bal, Electrospray-induced mass spectrometry is not suitable for determination of peptidic Cu (II) complexes, *J. Am. Soc. Mass Spectrom.*, 2021, **32**(12), 2766–2776.
60 M. Prudent and H. H. Girault, Functional electrospray emitters, *Analyst*, 2009, **134**(11), 2189–2203.
61 K. Matyjaszewski and J. Xia, Atom Transfer Radical Polymerization, *Chem. Rev.*, 2001, **101**(9), 2921–2990, DOI: 10.1021/cr940534g.
62 C. Liu, J. Liu, W. Li, H. Lu and Y. Zhang, Recent advances in electrochemical C–H bond amination, *Org. Chem. Front.*, 2023, **10**(20), 5309–5330, DOI: 10.1039/d3qo01159c.
63 Z.-L. Li, G.-C. Fang, Q.-S. Gu and X.-Y. Liu, Recent advances in copper-catalysed radical-involved asymmetric 1,2-difunctionalization of alkenes, *Chem. Soc. Rev.*, 2020, **49**(1), 32–48, DOI: 10.1039/c9cs00681h.
64 J. L. Ma, X. M. Zhou, P. H. Guo, H. C. Cheng and H. B. Ji, <scp>Copper-Mediated</scp> and Catalyzed C—H Bond Amination via Chelation Assistance: Scope, Mechanism and Synthetic Applications, *Chin. J. Chem.*, 2022, **40**(10), 1204–1223, DOI: 10.1002/cjoc.202100812.
65 Q.-L. Yang, X.-Y. Wang, J.-Y. Lu, L.-P. Zhang, P. Fang and T.-S. Mei, Copper-Catalyzed Electrochemical C–H Amination of Arenes with Secondary Amines, *J. Am. Chem. Soc.*, 2018, **140**(36), 11487–11494, DOI: 10.1021/jacs.8b07380.
66 J. L. Ma, X. M. Zhou, P. H. Guo, H. C. Cheng and H. b. Ji, Copper-Mediated and Catalyzed C—H Bond Amination via Chelation Assistance: Scope, Mechanism and Synthetic Applications, *Chin. J. Chem.*, 2022, **40**(10), 1204–1223.
67 Z. Wei, M. Wleklinski, C. Ferreira and R. G. Cooks, Reaction acceleration in thin films with continuous product deposition for organic synthesis, *Angew. Chem.*, 2017, **129**(32), 9514–9518.
68 H. Cheng, S. Tang, T. Yang, S. Xu and X. Yan, Accelerating electrochemical reactions in a voltage-controlled interfacial microreactor, *Angew. Chem., Int. Ed.*, 2020, **59**(45), 19862–19867.
69 P. W. Fedick, K. Iyer, Z. Wei, L. Avramova, G. O. Capek and R. G. Cooks, Screening of the Suzuki cross-coupling reaction using desorption electrospray ionization in high-throughput and in Leidenfrost droplet experiments, *J. Am. Soc. Mass Spectrom.*, 2019, **30**(10), 2144–2151.

70 R. L. Schrader, P. W. Fedick, T. F. Mehari and R. G. Cooks, Accelerated chemical synthesis: three ways of performing the Katritzky transamination reaction, *J. Chem. Educ.*, 2019, **96**(2), 360–365.
71 D. Avhad, A. Asnani, S. Mohurle, P. Kumar, A. Bais and R. Tale, Review on synthetic study of benzotriazole, *GSC Biol. Pharm. Sci.*, 2020, **11**(2), 215–225, DOI: 10.30574/gscbps.2020.11.2.0137.
72 A. R. Katritzky and S. Rachwal, Synthesis of Heterocycles Mediated by Benzotriazole. 1. Monocyclic Systems, *Chem. Rev.*, 2010, **110**(3), 1564–1610, DOI: 10.1021/cr900204u.
73 J. Zhou, J. He, B. Wang, W. Yang and H. Ren, 1,7-Palladium Migration via C–H Activation, Followed by Intramolecular Amination: Regioselective Synthesis of Benzotriazoles, *J. Am. Chem. Soc.*, 2011, **133**(18), 6868–6870, DOI: 10.1021/ja2007438.
74 X. Luo, A. Tian, M. Pei, J. Yan, X. Liu and L. Wang, Highly Stable Univalent Copper of a Cu@Al/SBA-15 Nanocomposite Catalyzes the Synthesis of Fluorescent Aminobenzotriazoles Derivatives, *Chem. – Eur. J.*, 2022, **28**(3), e202103361.
75 A. Kokel and B. Török, Microwave-assisted solid phase diazotation: a method for the environmentally benign synthesis of benzotriazoles, *Green Chem.*, 2017, **19**(11), 2515–2519, DOI: 10.1039/c7gc00901a.
76 C. Zhang and N. Jiao, Copper-catalyzed aerobic oxidative dehydrogenative coupling of anilines leading to aromatic azo compounds using dioxygen as an oxidant, *Angew. Chem.*, 2010, **35**(122), 6310–6313.
77 C. Zhang, C. Tang and N. Jiao, Recent advances in copper-catalyzed dehydrogenative functionalization via a single electron transfer (SET) process, *Chem. Soc. Rev.*, 2012, **41**(9), 3464–3484.
78 W. Lu and C. Xi, CuCl-catalyzed aerobic oxidative reaction of primary aromatic amines, *Tetrahedron Lett.*, 2008, **49**(25), 4011–4015.
79 A. Tabey, P. Y. Vemuri and F. W. Patureau, Cross-dehydrogenative N–N couplings, *Chem. Sci.*, 2021, **12**(43), 14343–14352.
80 J. A. Joule, K. Mills and G. F. Smith, *Heterocyclic Chemistry*, CRC Press, London, 3rd edn, 2020, DOI: 10.1201/9781003072850.
81 G. Dai, L. Yang and W. Zhou, Copper-catalyzed oxidative dehydrogenative N–N bond formation for the synthesis of N, N′-diarylindazol-3-ones, *Org. Chem. Front.*, 2017, **4**(2), 229–231.
82 C. Liu, D. Liu and A. Lei, Recent Advances of Transition-Metal Catalyzed Radical Oxidative Cross-Couplings, *Acc. Chem. Res.*, 2014, **47**(12), 3459–3470, DOI: 10.1021/ar5002044.
83 J. Yuan, C. Liu and A. Lei, Construction of N-containing heterocycles via oxidative intramolecular N–H/X–H coupling, *Chem. Commun.*, 2015, **51**(8), 1394–1409.
84 H. Wang, Y. Wang, C. Peng, J. Zhang and Q. Zhu, A Direct Intramolecular C–H Amination Reaction Cocatalyzed by Copper(II) and Iron(III) as Part of an Efficient Route for the Synthesis of Pyrido[1,2-a]benzimidazoles from N-Aryl-2-aminopyridines, *J. Am. Chem. Soc.*, 2010, **132**(38), 13217–13219, DOI: 10.1021/ja1067993.
85 D.-G. Yu, M. Suri and F. Glorius, RhIII/CuII-Cocatalyzed Synthesis of 1H-Indazoles through C–H Amidation and N–N Bond Formation, *J. Am. Chem. Soc.*, 2013, **135**(24), 8802–8805, DOI: 10.1021/ja4033555.